Cellular and Molecular Life Sciences (2025) 82:125
https://doi.org/10.1007/s00018-025-05658-0

ORIGINAL ARTICLE

R-spondins secreted by human pancreas-derived mesenchymal stromal cells support pancreatic organoid proliferation

Alessandro Cherubini[1] · Clelia Pistoni[2,3] · Maria Chiara Iachini[2] · Cecilia Mei[2,4] · Francesco Rusconi[2] · Valeria Peli[2] · Mario Barilani[2] · Dorian Tace[2] · Noemi Elia[2] · Fabio Lepore[5] · Vittoria Caporale[6] · Lorenzo Piemonti[7] · Lorenza Lazzari[2]

Received: 27 July 2024 / Revised: 28 February 2025 / Accepted: 11 March 2025

Abstract

Mesenchymal stromal cells (MSC) play a critical role in the stem cell niche, a specialized microenvironment where stem cells reside and interact with surrounding cells and extracellular matrix components. Within the niche, MSC offer structural support, modulate inflammatory response, promote angiogenesis and release specific signaling molecules that influence stem cell behavior, including self-renewal, proliferation and differentiation. In epithelial tissues such as the intestine, stomach and liver, MSC act as an important source of cytokines and growth factors, but not much is known about their role in the pancreas. Our group has established a standardized technology for the generation of pancreatic organoids. Herein, we investigated the role of pancreatic mesenchymal stromal cells in the regulation of human pancreatic organoid proliferation and growth, using this 3D model in a co-culture system. We particularly focused on the capacity of pancreatic MSC to produce R-spondin factors, which are considered critical regulators of epithelial growth. We propose the development of a complex in vitro system that combines organoid technology and mesenchymal stromal cells, thereby promoting the assembloid new research era.

Keywords Pancreas · Organoids · R-spondin · Mesenchymal stromal cells

Introduction

The pancreas is a heterocrine glandular organ of the digestive system involved in many homeostatic functions. In addition to the well-known insulin-producing beta cells, the endocrine pancreas contains several other hormone-secreting cell types, including alpha, gamma and delta cells, which play critical roles in maintaining glucose homeostasis and overall metabolic balance. Alpha cells secrete glucagon, a hormone that raises blood glucose levels by promoting glycogen breakdown in the liver. Delta cells produce somatostatin, which inhibits the release of both insulin and glucagon, as well as suppressing the secretion of digestive enzymes and other hormones. Gamma cells, also known as pancreatic polypeptide (PP) cells, release pancreatic polypeptide, which regulates both endocrine and exocrine pancreatic secretions and influences hepatic glycogen levels. These diverse cell types work in concert to ensure the precise regulation of metabolic processes and digestive functions within the pancreas [1].

Even if the pancreatic epithelium shows a low cellular turnover rate in normal conditions, it is capable of

Alessandro Cherubini, Clelia Pistoni and Maria Chiara Iachini equally contributed to this work.

✉ Lorenza Lazzari
lorenza.lazzari@policlinico.mi.it

1 Precision Medicine Lab-Department of Transfusion Medicine, Fondazione IRCCS Ca' Granda Ospedale Maggiore Policlinico, Milan, Italy

2 Unit of Cell and Gene Therapies, Fondazione IRCCS Ca' Granda Ospedale Maggiore Policlinico, Milan, Italy

3 Department of Medical Oncology and Hematology, University Hospital Zurich, Zurich, Switzerland

4 Department of Pathophysiology and Transplantation, Dino Ferrari Center, University of Milan, Milan, Italy

5 Laboratory of Cellular Therapies, Department of Medical and Surgical Sciences, University of Modena and Reggio Emilia, Modena, Italy

6 Laboratory of Transplant Immunology SC Trapianti Lombardia–NITp, Fondazione IRCCS Ca' Granda Ospedale Maggiore Policlinico, Milan, Italy

7 Diabetes Research Institute, IRCCS San Raffaele Scientific Institute, Milan, Italy

Published online: 20 March 2025

proliferating in response to damage, allowing for regeneration of both the endocrine and exocrine compartments [2, 3], suggesting the presence of an epithelial progenitor niche [4].

Indeed, stem cells reside in defined niches in the pancreas, where their self-renewal and differentiation are tightly regulated through the coordinated activity of several extrinsic factors [5–7]. These regulators include potent secreted molecules such as Hedgehogs, Notch ligands, Wnt ligands (WNTs), R-spondins (RSPOs), and others [8, 9]. One of the most important biological signals required to instruct pancreatic progenitor cells into a particular lineage during routine turnover, following injury, or during development, comes from the Wnt/β-catenin signaling cascade [10–12]. In the pancreas, it has been shown that some Wnt responses depend on an agonistic second signal provided by the RSPO protein family, which comprises secreted proteins that bind to the leucine-rich repeat-containing G protein-coupled receptor (LGR) 5 [13–15]. RSPO activator proteins amplify Wnt signal by the inactivation of two transmembrane E3 ubiquitin ligases, ZNRF3 and RNF43, which reduce cell-surface levels of WNT receptors via ubiquitination-mediated degradation favoring cell proliferation [16–19].

The concept of "stem cell niche" was first proposed by R. Schofield, who suggested the existence of a microanatomical structure in which the microenvironment determines the behavior of the stem cells [20]. It has been shown that this niche not only maintains stem cells but can also stimulate progenitor cell differentiation and, under certain conditions, revert them to an undifferentiated state. [21–23]. Presumably, maintaining stem cells and transferring their properties to niche cells may be an important aspect of damaged tissue regeneration, since they can be recruited to restore tissue. In the majority of stem cell niches, mesenchymal stromal cells (MSC) meet these requirements [24–27]. Since stromal compartments are present in almost all the organs, MSC are known to be isolated from various adult tissues, like bone marrow [28] and adipose tissue [29], as well as neonatal tissues, i.e. cord [30] and cord blood [31, 32]. MSC maintain and regulate cellular behavior in the microenvironment by secreting various growth factors and cytokines. They also have the ability to modify and regulate their secretion and signals in respond to damage, for example, by changing the number and panel of secreted factors [33, 34]. This may also be one of the strategies through which MSC regulate the behavior of stem cells in a niche, and ultimately promote tissue regeneration [35].

Recently, it has been demonstrated that the stromal compartment is also involved in the support of pancreatic physiological homeostasis [36, 37]. The presence of pancreatic MSC has been confirmed by a recent publication of one of the authors demonstrating that "the mesenchymal cells appearing from pancreatic tissue culture are not derived from an epithelial to mesenchymal transition, but are rather the expansion of a pool of resident MSCs" [38].

Recently, our group developed a pancreatic organoid technology that mainly represents the exocrine compartment of the pancreas. We derived human pancreatic organoids (hPO) from tissue-resident adult stem cells (AdSC) sourced from non-transplanted pancreatic fractions resulting from islet cell processing [39–43]. Pancreatic exocrine cells can be cultured and expanded in vitro as self-renewing 3D organoids (hPO) in presence of a basement membrane matrix and a specific cytokines cocktail, including R-spondin-1 (RSPO1), Noggin (NOG), Fibroblast Growth Factor 10 (FGF10) and epidermal growth factor (EGF) [39, 41, 42]. The potential of this technology ranges from basic research to exploring the biology of normal and tumor tissues, to translational medicine, where these 3D structures can be used for drug discovery and toxicity, hereditary diseases and personalized medicine studies. Despite their potential, nowadays, organoids still present limitations, among which are the inclusion of key cell types of the represented organ, such as stromal cells.

Herein, we analyzed the role of human pancreatic mesenchymal stromal cells (hPMSC) in the regulation of proliferation and growth of exocrine epithelial cells in pancreatic organoids, elucidating the crucial role of mesenchymal cell-secreted mitogens in the support of hPO formation and expansion.

Materials and methods

Pancreatic mesenchymal cell isolation and culture

Human pancreatic mesenchymal stromal cells (hPMSC) were isolated from healthy donors ranging from 55 to 63 years old (Table S1). Digested pancreatic tissue was placed into minimum essential medium (αMEM; ECM0849L; Euroclone) supplemented with 1% Penicillin–Streptomycin (15,070,063; Gibco), 1 × GlutaMAX™ (A1286001; Gibco) and 10% FBS (32,561,037; Thermo Fisher Scientific) to select the pancreatic mesenchymal cell population. Cell cultures were maintained at 37 °C with 5% CO_2 in a humidified atmosphere. At 80% confluence, cells were harvested using TrypLE™ Select enzyme (12,604,013; Gibco) and seeded at 5×10^3 cells/cm^2 for expansion. Medium changes were performed twice a week with the same isolation medium. hPMSC were fully characterized for appropriate MSC identity following the International Society for Cellular Therapy guidelines [43, 44].

hPMSC differentiation

Differentiation capacity of hPMSC was assessed using commercial media (Lonza), following the manufacturer's protocols. Human MSC adipogenesis induction medium (PT-3102B; Lonza) and maintenance medium (PT-3102A; Lonza) were used to induce adipogenesis; oil red O solution (O0625; Sigma-Aldrich) was used to stain lipid vacuoles as previously shown [45]. Human MSC Osteogenic Medium (PT-3002; Lonza) was used to induce osteogenesis; calcium deposits were stained with Alizarin Red S (A5533; Sigma-Aldrich) as previously shown [32]. Images of stained cells were taken with a Nikon Eclipse TS100 microscope (Nikon).

Pancreatic organoids culture

Human pancreatic organoids (hPO) were obtained from the same 5 independent healthy donors as hPMSC. hPO were isolated as previously described [39]; briefly, raw material was digested in 0.125 mg/mL Liberase MTF C/T (5,339,880,001; Roche), 0.125 mg/mL neutral protease (30303.01; Serva), and 0.1 mg/mL DNase I (3,724,751,103; Roche) in human complete medium at 37 °C for ≤ 2 h [46]. Resulting pancreatic cell clumps were embedded in 100% Cultrex Basement Membrane Extract (BME), Type 2 (3532-010-02; Bio-techne) and cultured in Expansion medium, which includes human complete Advanced DMEM/F-12 (12,634,010; Thermo Fisher Scientific) supplemented with 1 × HEPES (15630-106; Gibco), 1 × GlutaMAX™ (A1286001; Gibco), 1% Penicillin–Streptomycin (15070-063; Gibco), 1 × B27 minus Vitamin A (12587-010; Gibco), 1 × N2 supplement (17502-048; Gibco), 1 mM N-acetyl-L-cysteine (A9165; Sigma-Aldrich), 1 µg/mL R-spondin-1 (RSPO1) recombinant protein (120-38; Peprotech) or RSPO1 conditioned medium [47], 0.1 µg/mL Noggin recombinant protein (120-10C; Peprotech), 50 ng/mL epidermal growth factor (EGF, 100-15; Peprotech), 10 nM gastrin (G9145; Sigma-Aldrich), 100 ng/mL fibroblast growth factor 10 (FGF10, 100-26; Peprotech), 10 mM nicotinamide (N0636; Sigma-Aldrich), 10 µM forskolin (1099; Tocris Bioscience), 3 µM Prostaglandin E2 (PGE-2, 2296; Tocris Bioscience), and 0.5 µM A83-01 (9,094,360; Peprotech). After isolation, hPO cultures were maintained at 37 °C with 5% CO_2 in a humidified atmosphere. The medium was changed every 3–4 days and hPO were split every 7–8 days.

hPMSC and hPO co-culture

For transwell-based co-cultures, hPMSC were seeded on the bottom of 24-well plates (83.3922; Sarstedt) at a density of 30,000 cells per well. hPO fragments were then seeded onto the top of 0.4 µm pore size transwell inserts (83.3932.041; Sarstedt) within a 40 µL drop of 100% Cultrex Basement Membrane Extract (BME), Type 2 (3532-010-02; Bio-techne). CC3 medium containing Advanced DMEM/F-12 (12,634,010; Thermo Fisher Scientific), 1 × HEPES (15630-106; Gibco), 1 × GlutaMAXTM (A1286001; Gibco), 1% Penicillin–Streptomycin (15070-063; Gibco), 1 × B27 minus Vitamin A (12587-010; Gibco), 1 × N2 supplement (17502-048; Gibco), 1 mM N-acetyl-L-cysteine (A9165; Sigma-Aldrich) and 3% FBS (32,561,037; Thermo Fisher Scientific) was used to sustain cell growth. Co-culture was maintained for 7 days at 37 °C with 5% CO_2 in a humidified atmosphere. Successively, hPO and hPMSC were separately collected for further analysis.

DNA extraction

DNA extraction was performed as reported: first hPO or hPMSC cells were collected and washed with PBS. All the samples were lysed overnight at 37 °C, under rotation, in 1.1 mL of lysis buffer (EDTA, pH: 8, 10 mM; TRIS, pH: 7.44, 20 mM; NaCl, 100 mM) containing 50 µL of DNA PK (1 mg/ml) and 300 µL of 10% SDS. The day after an equal volume of Phenol: Cloroform: Isoamyl Alchohol 25: 24: 1 v/v (Merck, Cat. No 516726-1SET) was added and, post a centrifugation step (5 min at 7800 G) the upper phase was taken. This passage was repeated twice. Afterwards an equal volume of CIAA (Clorofom: Isoamyl Alchohol, Merck, Cat. No 25666-100ML) was added and, after centrifugation (5 min at 7800 G) only the upper phase was used. The precipitation of DNA was performed at −80 °C for 30 min adding to all samples 0.1 v/v of NaCl 5 M and 1.5 v/v of absolute ethanol. After a centrifugation step (15 min at 13,800 G at 4 °C) DNA pellets were washed with 70% ethanol and centrifuged for 5 min at 13,800 G at 4 °C. Finally, every pellet was resuspended in an adequate volume of water (50 or 100 µL). Before the quantification step (performed with NanoDrop) all samples were at 60 °C for 15 min to remove residual ethanol.

Short tandem repeat analysis

DNA samples, isolated from hPO and hPMSC, were quantified using a NanoDrop and diluted to the final concentration of 0.08 ng/ml. PCR reactions and electrophoresis were run on Applied Biosystems 3500 Genetic Analyzer and carried out according to manufacturer's instructions. More precisely, the AmpFℓSTR™ Identifiler™ Plus PCR Amplification Kit (Applied Biosystems, Thermo Fisher) was used. 15 short tandem repeat loci (D8S1179, D21S11, D7S820, CSF1PO, D3S1358, TH01, D13S317, D16S539, D2S1338, D19S433, vW, TPOX, D18S51, D5S818, FGA) and a segment of the X–Y homologous gene amelogenin were amplified. GeneMapper software automatically analyzed the collected data

that were compared to establish the genotypic identity of our samples.

Quantitative real-time PCR

Total RNA was extracted from both hPO and hPMSC with TRIzol reagent (15,596,026; Ambion), according to the manufacturer's instructions. Total RNA was quantified, and quality checked by NanoDrop ND-1000 spectrophotometer (NanoDrop Technologies, Wilmington, DE, USA). For the quantitative reverse transcription-polymerase chain reaction (qRT-PCR) assay, cDNA was synthesized with SuperScript IV VILO Master Mix (11,756,050; Thermo Fisher Scientific). The resulting cDNA was diluted 1:10 in water and 1 µL was used as a template for qRT-PCR analysis with PowerUp SYBR Green Master Mix (A15780; Applied Biosystems) in a CFX96 thermal cycler (BioRad). For each primer pair used the sequence is shared in Table S2. Relative gene expression levels were determined with the $-\Delta Ct$ method; data were normalized to geometric means of endogenous ACTB, GAPDH and TBP mRNA levels.

Flow cytometry

Human pancreatic organoids were disaggregated by trypsinization with Trypsin (37,297.01; SERVA, Germany) at 37 °C for 15 min, pipetting every 5 min, or until single cell suspension was obtained. Next, cells were centrifuged for 5 min at 350 × g and resuspended in PBS w/o Ca^{2+} and Mg^{2+} (D8537; Sigma-Aldrich). Human mesenchymal cells were instead harvested using TrypLE™ Select enzyme (12,604,013; Gibco). Single cell assessment and cell count were performed using a hemocytometer. To detect surface markers, 100,000 cells were incubated with fluorophore-conjugated antibodies anti-human CD34 (345,802; BD Biosciences), CD45 (641,417; BD Biosciences), CD90 (561,558; BD Biosciences), CD73 (560,847; BD Biosciences), CD105 (560,819; BD Biosciences), in a total volume of 200 µL of PBS w/o Ca^{2+} and Mg^{2+} (D8537; Sigma-Aldrich) for 20 min in the dark at room temperature, washed with 3 mL of PBS w/o Ca^{2+} and Mg^{2+} (D8537; Sigma-Aldrich) and resuspended in 200 µL of PBS w/o Ca^{2+} and Mg^{2+} (D8537; Sigma-Aldrich) for analysis. To detect intracellular markers, 100,000 cells were fixed with PFA 2% (P6148; Sigma-Aldrich) in a total volume of 200 µL for 15 min at room temperature. Cells were further washed with PBS w/o Ca^{2+} and Mg^{2+} (D8537; Sigma-Aldrich). Cells were then incubated at 37 °C for 30 min in 200 µL of PBS w/o Ca^{2+} and Mg^{2+} (D8537; Sigma-Aldrich) containing saponin 0.05% (47,036; Sigma-Aldrich), 10% FBS (32,561,037; Thermo Fisher Scientific) and the primary antibody against KRT19 (sc-5300; Santacruz), AMY2B (PA5-24,187; Invitrogen) and MUC1 (sc-7313; Santacruz). Cells were then washed with PBS w/o Ca^{2+} and Mg^{2+} (D8537; Sigma-Aldrich) and further incubated for 10 min at room temperature in 200 µL of PBS w/o Ca^{2+} and Mg^{2+} (D8537; Sigma-Aldrich) containing saponin 0.05% (47,036; Sigma-Aldrich), 10% FBS (32,561,037; Thermo Fisher Scientific) and secondary antibody goat anti-mouse (F-2761; Invitrogen) and goat anti-rabbit (L43018; Invitrogen). Cells were washed with PBS w/o Ca^{2+} and Mg^{2+} (D8537; Sigma-Aldrich) and resuspended with PBS w/o Ca^{2+} and Mg^{2+} (D8537; Sigma-Aldrich) for analysis. The samples were analyzed using a BD FACSCanto II cytometer and the BD FACSDiva analysis software (BD). Acquired events were plotted against forward and side scatter area physical parameters and a homogenous cell population was selected (P1 gate) excluding debris. At least 10,000 P1 events were acquired.

MTT assay

hPMSC were washed twice with PBS w/o Ca^{2+} and Mg^{2+} (D8537; Sigma-Aldrich) and 0.5 mg/mL of thiazolyl blue tetrazolium bromide (M5655; Sigma-Aldrich) dissolved in DMEM w/o phenol red (D1145; Sigma-Aldrich) were added to each well (working MTT solution). Regarding hPO instead, the culture medium was removed and the solution of thiazolyl blue tetrazolium bromide was directly added to the well containing organoids in the Cultrex® BME drop. Cells or organoids were then incubated in the dark at 37 °C with 5% CO_2 in a humidified atmosphere for 2 h. Next, the MTT solution was removed and 300 µL of 96% ethanol (528,151; Carlo Erba) was added to each well. Plates were next placed on a rocking shaker at 37 °C with 5% CO_2 in a humidified atmosphere for 30 min for hPMSC and for at least 2 h for hPO. Optical density was measured at 570 nm on a GENios microplate reader (TECAN).

Western analysis

Organoids were disrupted using cold PBS w/o Ca^{2+} and Mg^{2+} (D8537; Sigma-Aldrich) by pipetting 10 times with a 1000 µL tip. Then, organoid fragments were centrifuged for 5 min at 350 × g and lysed in F-buffer containing 1% Triton X-100 (GAUTTR0001; Eurobio Scientific), 10 mM Tris–HCl pH 7 (93,362; Sigma-Aldrich), 100 mM NaCl (S7653; Sigma-Aldrich), 30 mM $Na_4P_2O_7$ (P8010; Sigma-Aldrich), 50 mM NaF (201,290,025; Thermo Fisher Scientific), 85 mM $ZnCl_2$ (424,595,000; Acros Organics B.V.B.A.), 1 × protease/phosphatase mix inhibitor (P8340; Sigma-Aldrich) for 20 min on ice. The lysate was centrifuged for 5 min at 350 × g and the supernatant collected for protein dosage by BCA assay (23,227; Thermo Fisher Scientific). For western analysis, 15 µg of protein samples were boiled and loaded onto a pre-cast 4%–20% Tris–glycine gel (XP04202BOX; Thermo Fisher Scientific) and run

in Tris/Glycine/SDS Buffer (1,610,772; Bio-Rad). After electrophoresis, proteins were transferred to a nitrocellulose membrane (IB23001; Thermo Fisher Scientific). Membranes were blocked with 5% non-fat dried milk (10,004,504; Bio-Rad), in TBS (1,706,435; Bio-Rad), containing 0.1% or 0.05% of Tween 20 (P1379; Sigma-Aldrich), depending on the manufacturer's instructions for each specific antibody. Membranes were then incubated overnight at 4 °C with primary antibodies anti- keratin, type I cytoskeletal 19 (SC-53003; Santa Cruz Biotechnology), alpha-amylase 2B (PA5-24,187; Thermo Fisher Scientific), Mucin-1 (SC-7313; Santa Cruz Biotechnology) and glyceraldehyde-3-phosphate dehydrogenase (SC-47724; Santa Cruz Biotechnology). After 2 h of incubation with secondary antibodies, the proteins of interest were visualized with Pierce ECL Western detection kit (32,106; Thermo Fisher Scientific) or ECL ultra-sensitive reagent (WBULS0500; Millipore, Burlington, MA, USA). Chemiluminescence images were obtained on a ChemiDoc XRS + system (Bio-Rad).

TOP-FOP assay

To demonstrate that pancreatic stromal cells produce factors related to the Wnt canonical pathway, a TOP-FOP luciferase assay was performed testing fresh CC3 medium and 1 week-old hPMSC CC3 conditioned medium. In summary the TOP-FOP assay was performed as described below. First, HEK-293T cells were seeded in 24-well plates ($8*10^5$ cells/well) at 24 h prior to transfection. Then, the cells were co-transfected (per well) with 20 ng PGL4.24 *luc*2P and 180 ng of TOPflash reporter vector or 180 ng FOPflash reporter vector as negative control. After 24 h, the HEK-293T cell culture medium was replaced with the hPMSC conditionate medium or fresh CC3 medium. The day after, cells were collected and processed using the Dual-Luciferase Reporter Assay System (E1910; Promega) following manufacturer instructions. For every sample luciferase activity was measured using an infinite F200 pro (TECAN).

ELISA assay

To confirm that hPMSC are able to produce and secrete RSPO1 and RSPO3 aliquots of conditioned culture media were collected and tested with ELISA assays following manufacturer's instructions (HUDL02571; Assay Genie for RSPO1 and OKBB01047; Aviva System Biology for RSPO3). More precisely, for each test, one week-old CC3 and one week-old MSC standard medium were collected and used to perform the tests.

Immunofluorescence and confocal microscopy

hPMSC were isolated from digested pancreatic tissue, as previously described, and cultured in Falcon 4-well culture slides (354,114; Corning). As soon as they reached 70% confluency, without any passage, cells were incubated at 37 °C overnight with 10 µg/mL Brefeldin A (S7046; Selleckchem).

Samples were fixed in 4% paraformaldehyde (SC-201692; ChemCruz) for 20 min on ice, washed and permeabilized for 30 min in 0.3% Triton X-100 (GAUTTR0001; Eurobio Scientific), 3% Bovine Serum Albumin (P6156; Biowest). Then, cells were incubated with rabbit anti-human RSPO1 1:100 (orb526678; Biorbyt), and mouse anti-human Vimentin 1:250 (CBL202-K; Sigma-Aldrich) primary antibodies overnight at 4 °C. The day after, cells were incubated with anti-rabbit Alexa Fluor-488 1:250 (A11008; Thermo Fisher Scientific) and anti-mouse Alexa Fluor-555 1:250 (A21422; Thermo Fisher Scientific) secondary antibodies for 1 h at room temperature and with 0.1 µg/mL DAPI (1,023,627,600; Roche). Culture slides were mounted on ProLong Glass Antifade Mountant (P36984; Thermo Fisher Scientific).

Immunofluorescence imaging was performed using a Leica SP8 Stellaris confocal microscope (Leica, Wetzlar, Germany), managed by LASX software. The acquisition was taken with a white light laser and Diode 405, using the HC PL APO CS2 20X/0.75 DRY NA and the HC PL APO CS 2 63X/1.30 GLYC NA objectives.

Neutralizing antibody functional assay

hPO and hPMSC were co-cultured in CC3-medium, at day 0 and day 4 supplemented with 3–12 µg/mL anti-RSPO1 antibody (Human R-Spondin 1 Antibody Antigen Affinity-purified Polyclonal Sheep IgG AF4645; R&D, Bio-Techne). Untreated co-culture was used as controls. After 7 days, a MTT assay on hPO and hPMSC was performed to evaluate their metabolic activity. hPMSC were treated as previously described (MTT assay), whereas for hPO a slightly different protocol was applied. Briefly, 200 µL of working MTT solution were added on top of the transwells, which were then incubated in the dark at 37 °C with 5% CO_2 in a humidified atmosphere for 2 h. Next, the MTT solution was removed and 200 µL of 96% ethanol (528,151; Carlo Erba) was added to each well. Plates were next placed on a rocking shaker at 37 °C with 5% CO2 in a humidified atmosphere for at least 2 h to ensure optimal resuspension of the MTT solution. Optical density was measured at 570 nm on a GENios microplate reader (TECAN).

Data analysis and visualization

Publicly available scRNA-seq datasets were downloaded from the Gene Expression Omnibus (GEO) [48–51]. The

Seurat version 4.2.3 R toolkit was used for scRNA-seq data analysis due to its ability to integrate across datasets, following the pipeline outlined by the package developers [52, 53]. To normalize the data, UMI counts were scaled by library size and a natural log transformation using NormalizeData() function. Integration of 4 scRNA-seq datasets on one hand was achieved by running consecutively FindIntegrationAnchors() and IntegrateData() functions from Seurat, with 2000 integration features. Then PCA was computed and the first 30 PCs were inputted for uniform manifold approximation and projection (UMAP) of integrated scRNA-seq datasets. Next, to identify clusters within the reduced dimensional space, cells were embedded in a k-nearest neighborhood-based graph structure by FindNeighbors() function and an unsupervised clustering was performed using FindClusters() function with Louvain algorithm (resolution = 0.4). The cells were then labelled according to the expression of specific markers.

Statistical analysis

All the quantitative data are shown as means ± SD, as indicated in each figure legend with the specific statistical test used. All experiments were repeated at least three times, each performed on samples from five different donors, as reported in each figure legend. All statistical tests were performed using Prism 8 and statistical significance (p-value) in figure asterisks mean *P < 0.05, **P < 0.01, ***P < 0.001. P values < 0.05 were considered significant, while P values > 0.05 were not reported.

Results

Isolation of syngeneic human pancreatic mesenchymal stromal cells and organoids

To mimic the closest setting to physiological conditions, syngeneic cell types were generated from 5 independent healthy donors (Table S1).

Syngeneic human pancreatic organoids and mesenchymal cells were isolated from the same islet-depleted digested (< 1% endocrine tissue) pancreatic tissue (Fig. 1a). For hPO, isolated ductal fragments were embedded in Cultrex® BME and cultured in presence of a specific cytokine cocktail. Characteristic 3D cyst-like structures were established in 12 days (Fig. 1b, upper panels). For hPMSC isolation, minced tissues were cultured in a specific fibroblast medium, such as α-MEM supplemented with 10% FBS. Under these conditions, part of the cells adhered to the plate and a homogeneous monolayer with mesenchymal morphology was obtained within 12 days (Fig. 1b, lower panels).

As previously observed [39, 40], hPO showed a phenotypically heterogeneous cell population expressing KRT19, MUC1 and AMY2B, whereas the mesenchymal and endothelial compartments were absent (Fig. 1c, upper panel). Instead, according to the definition of the International Society for Cell Therapy [54], hPMSC expressed the canonical surface antigens of mesenchymal cells (CD73, CD90 and CD105), while they were negative for epithelial and hematopoietic markers (Fig. 1c, lower panel). Molecular analysis of cell type-specific markers of epithelial, mesenchymal, and endothelial compartments confirmed our immunophenotyping results (Supplementary Fig. 1a). To corroborate mesenchymal cell behavior and to confirm their mesenchymal nature, we successfully induced their differentiation toward osteoblast-like and adipocyte-like cells, following standard in vitro differentiation conditions. Molecular analysis confirmed hPMSC ability to undergo osteogenic and adipogenic differentiation pathways, as supported also by the Alizarin Red and Oil Red O staining (Supplementary Fig. 1b, c), assessing their mesenchymal multipotent identity.

DNA profiling (Supplementary Fig. 1d) showed that syngeneic hPMSC and hPO exhibit proper identity features and that they were consistently isolated from the same pancreatic samples, allowing for the study of their interactions without any biases potentially coming from the use of unrelated donors.

Human pancreatic mesenchymal cells possess a hPO growth-supporting secretory profile

To evaluate the relevance of different cytokines and growth factors in the support of pancreatic epithelial growth and homeostasis, using a human adult pancreas 3D model system, we decided to investigate if and how the absence of each crucial molecule contained in the organoid expansion medium would impair the metabolic activity of hPO. Interestingly, after 7 days, organoids grown in absence of RSPO1 showed a 50% viability impairment (Fig. 2a). Furthermore, hPO grown in absence of RSPO1 failed to survive more than two passages, observations which highlight the crucial role of this secreted protein on the maintenance of organoid cultures. Moreover, the absence of NOG was restrictive to support hPO growth (50% of viability), but the culture could be easily propagated for more than 3 weeks. The absence of no other growth factor or cytokine impaired the growth of organoids in a significant way over 21 days of culture (Fig. 2a).

We also wanted to gain a broad and complete picture of mesenchymal cell secretory landscape, to evidence their ability to produce and provide our growth factors of interest (proteins involved in the Wnt/β-catenin and Bone Morphogenetic Protein (BMP) signaling pathways) to the pancreatic

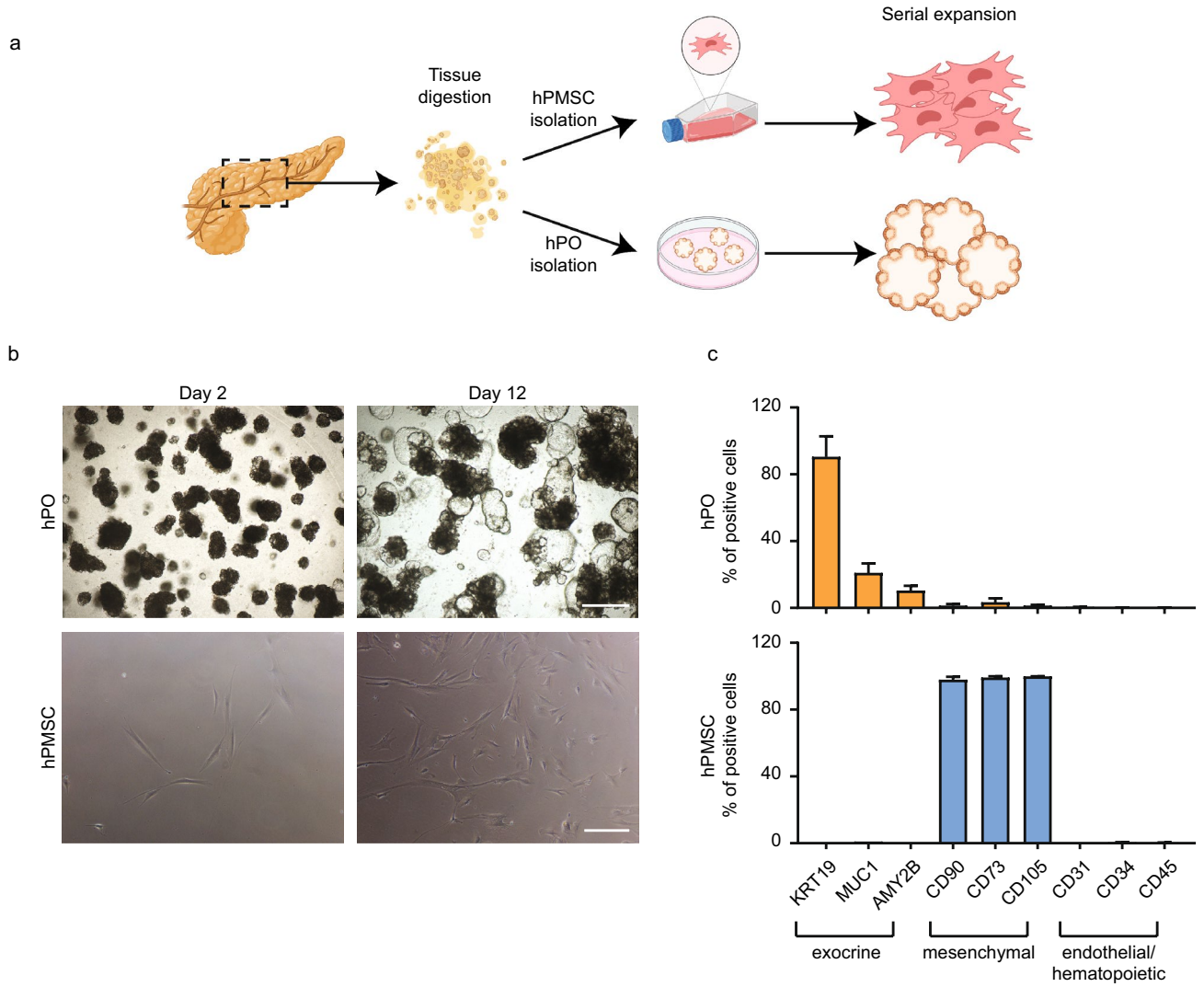

Fig. 1 Human pancreatic organoids and mesenchymal stromal cells isolation. **a** Schematic representation of isolation strategy for human pancreatic organoids (hPO) and human pancreatic mesenchymal stem cells (hPMSC). Created with BioRender.com. **b** Representative bright-field images of hPO and hPMSC after 2 (left) or 12 (right) days from isolation. Scale bar, 500 µm for hPO and 200 µm for hPMSC. **c** Flow cytometry analysis of hPO and hPMSC focused on exocrine, mesenchymal, endothelial and hematopoietic markers. Data are means ± SD ($n = 3$ independent experiments, each performed on samples from five different donors)

epithelial compartment. For this reason, four published whole pancreas single cell datasets were integrated and analyzed [48–51]. First, we clustered and plotted the combined datasets showing that all pancreatic cell types were largely preserved upon integration (Supplementary Fig. 2a-c). Interestingly, in pancreatic tissues, RSPO1 and RSPO3 resulted exclusively expressed by mesenchymal cells (Fig. 2b), while BMP related cytokines were expressed more heterogeneously among all pancreatic cells (Supplementary Fig. 2d).

Considering the highly relevant data that emerged from the previous wet and in silico analyses, we decided to investigate the actual capacity of our hPMSC and hPO to produce RSPO family factors and BMP-pathway protein inhibitors. In Fig. 2c we showed that hPMSC highly express Gremlin-1 and −2, members of the DAN family, and Noggin, another BMP antagonist. Some of these genes involved in the BMP signaling pathway did not present a restricted expression in hPMSC, which was instead also shared by hPO (Fig. 2c). Additionally, our findings indicated that certain genes belonging to the R-spondin protein family, which play a crucial role in the Wnt/β-catenin signaling pathway, were either uniquely or notably highly expressed in hPMSC compared to hPO. Interestingly, we also observed that the WNT receptor Lgr5 gene was expressed only in hPO (Fig. 2c). Supporting the idea that hPMSC play a pivotal role to support the homeostasis of the exocrine component of the pancreas.

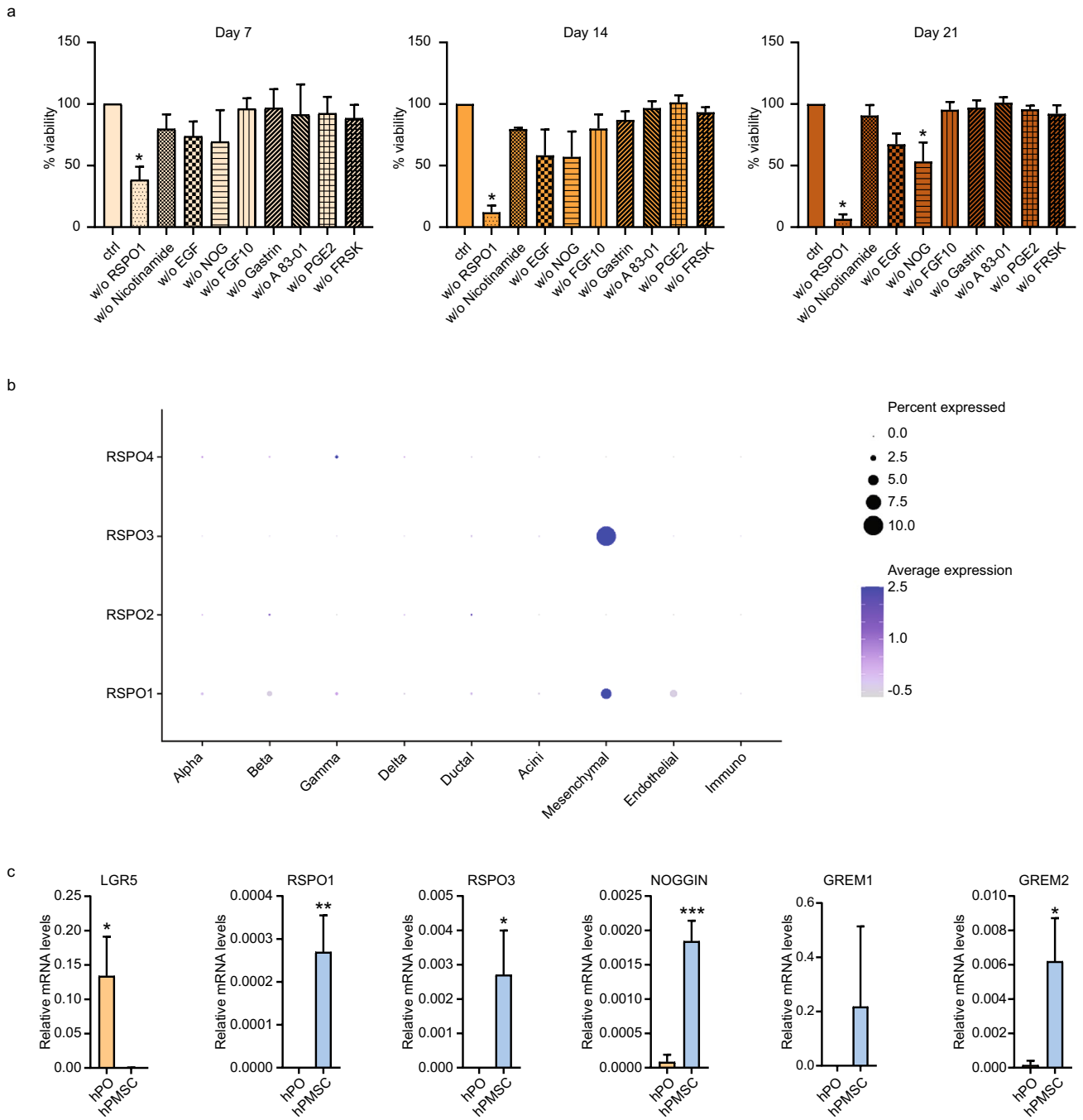

Fig. 2 RSPO-dependent WNT/β-Catenin signaling is dispensable for hPO expansion. **a** Cell viability of hPO in absence of specific factors at day 7, 14 and 21 after seeding. **b** Dot plot summarizes the expression of RSPO family genes within the pancreatic context. The size of the dot represents the percentage of cells expressing the marker genes, while the color of the dot indicates the average expression of the marker genes across all cells. **c** Relative expression of WNT and BMP related genes in hPO and hPMSC. Data are means ± SD ($n = 3$ independent experiments, each performed on samples from five different donors). **a** A one-way ANOVA was used followed by Dunnet test, * $p < 0.05$. **c** A two-sided, unpaired Student's t-test was used, * $p < 0.05$, ** $p < 0.01$, *** $p < 0.001$

Taken together, these results support the importance of the WNT/RSPO axis between mesenchymal and exocrine

cells as essential for pancreatic parenchymal regeneration and growth support.

Addition of human primary pancreatic mesenchymal stromal cells to 3D culture of human healthy pancreatic epithelial cells increased organoid development and proliferation

To investigate whether our hPMSC were able to effectively sustain the growth of hPO, we set up a transwell-based co-culture system. First, we identified the best basal medium, which supported the maintenance of both hPMSC and hPO, without having harmful effects on either the mesenchymal or the parenchymal component of the co-culture. To begin with, we grew hPMSC in 3 different conditions: AdDMEM/F12 supplemented with N2, B27, N-acetyl-cysteine and either no additional component (CC1), WNT3A 0.5 nM (CC2) or 3% FBS (CC3). After 7 days of culture CC3 medium was selected to set up the co-culture, since it showed a cell viability very close to the hPMSC cultured in Normal medium (Supplementary Fig. 3a, b); furthermore, hPMSC cultured in CC3 medium maintained the same morphology and expressed the same cell markers in normal mesenchymal medium (Supplementary Fig. 3c, d).

Next, hPMSC were seeded at the bottom of a 24-well plate, whereas hPO fragments were seeded within a Cultrex® BME drop deposited onto the top of a transwell insert. Both the bottom of the well and transwell were filled with CC3 medium, to allow the exchange of factors between hPO and hPMSC (Fig. 3a). After 7 days of co-culture, hPO retained the classical defined cystic structure, consisting of a proliferating cell monolayer. This morphology was completely in line with control hPO grown in standard expansion medium (Fig. 3b), consistent with previous observations [39, 55]. Interestingly, only a few aggregates characterized by small dimensions were observed when cultured in CC3 medium without mesenchymal cells (Fig. 3b), making it impossible to obtain RNA and proteins in sufficient quantity and quality for any analysis.

Thereafter, we determined the identity of hPO co-cultured in the presence of mesenchymal cells: hPO co-cultured with hPMSC showed a highly similar intracellular expression of ductal pancreatic markers compared with hPO maintained under standard expansion medium (Fig. 3c), while other markers such as AMY2B showed a slight increase level.

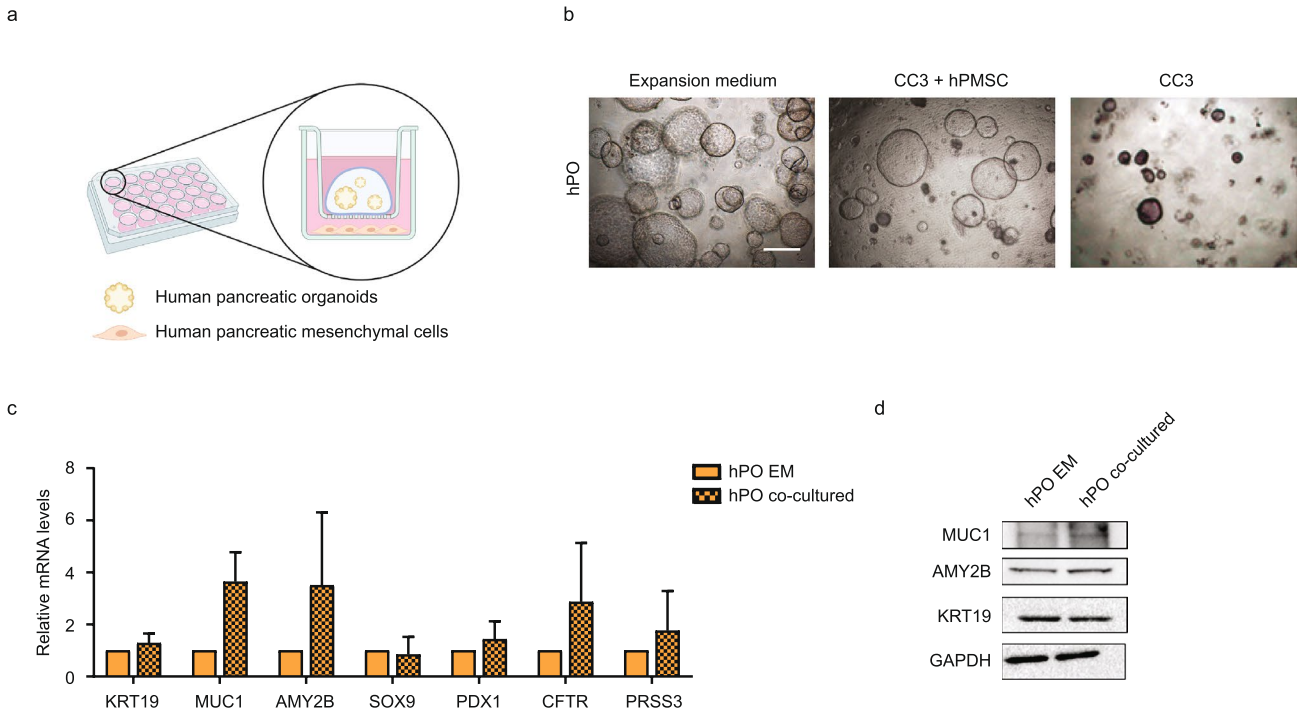

Fig. 3 hPMSC support hPO development in culture. **a** Schematic representation of co-culture setting, hPMSC were seeded at the bottom of 24 wells plate, hPO were seeded at the top of the transwell system allowing the exchange of growth factors and secreted proteins. Created with BioRender.com. **b** Representative bright-field images of hPO grown in standard expansion medium, in CC3 medium supported by hPMSC and in CC3 medium alone. Scale bar, 500 µm. **c** Relative expression analysis of acinar and ductal markers in hPO cultured in standard medium and hPO cultured in CC3 medium supported by hPMSC. **d** Western blot analysis of acinar and ductal markers of hPO cultured in standard medium and hPO cultured in CC3 medium supported by hPMSC. Data are means ± SD ($n = 3$ independent experiments, each performed on samples from five different donors)

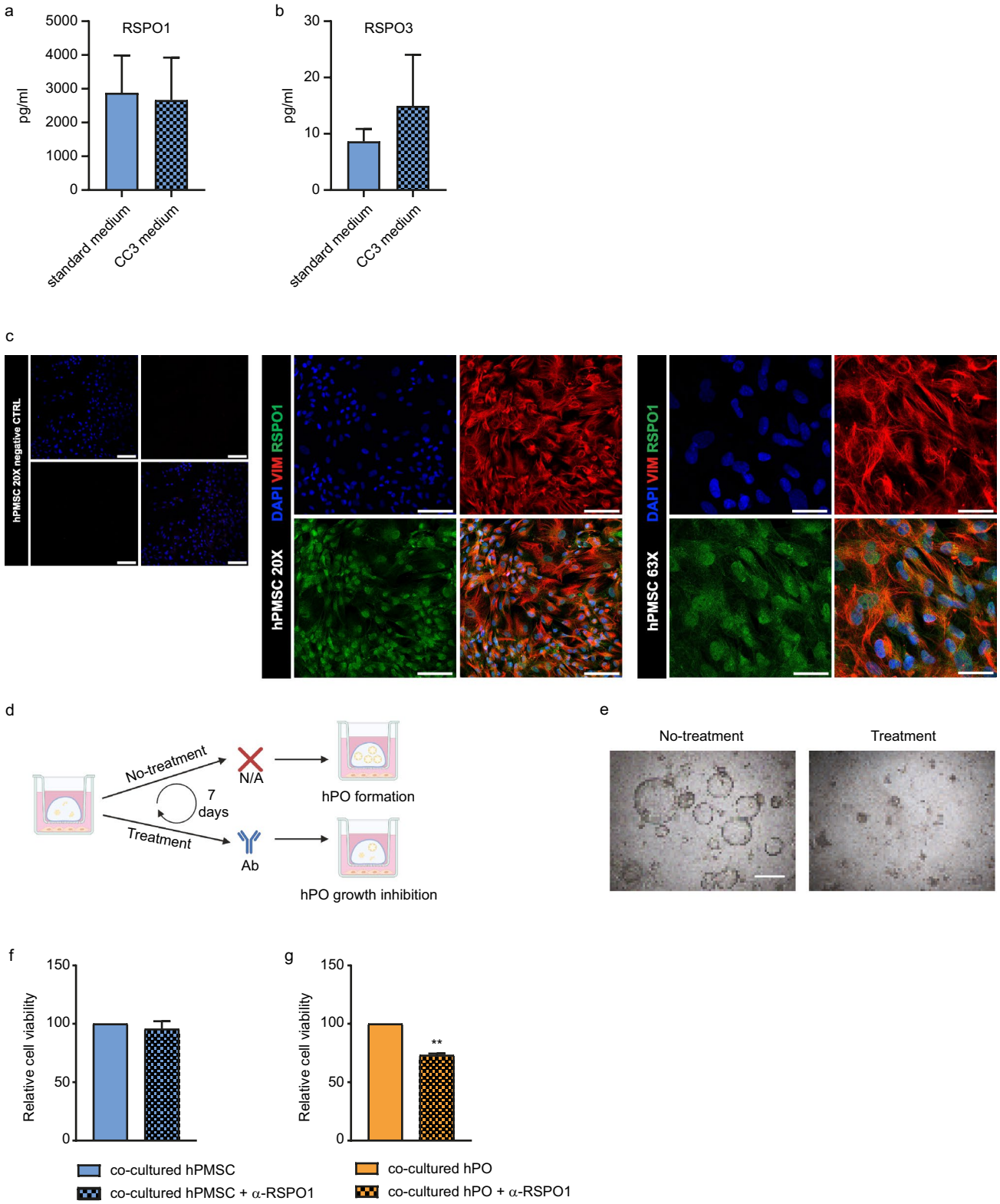

Moreover, western blot analysis for exocrine markers also confirmed a strong similarity of protein expression profiles between hPO grown in co-culture conditions and hPO grown in the expansion medium (Fig. 3d).

Overall, these results highlighted the robustness and relevance of hPMSC trophic support in sustaining organoid formation and proliferation in the same fashion as the standard cytokine-rich medium.

◂**Fig. 4** hPMSC-derived RSPO proteins are necessary for hPO expansion. **a**, **b** Concentration of RSPO1 and RSPO3 (expressed in pg/ml) secreted by hPMSC in both MSC standard medium and CC3 medium after seven days of culture. **c** Confocal microscopy images show representative fluorescent signals from DAPI (405, shown in blue), Vimentin (555, shown in red) and RSPO1 (488, shown in green) of hPMSC isolated from pancreatic digested tissue. Scale bars, 100 µm for 20X objective and 30 µm for 63X objective. **d** Schematic representation of neutralizing antibodies experiment set up. Created with BioRender.com. **e** Representative bright-field images of hPO treated or non-treated with neutralizing antibody against RSPO1. Scale bar, 500 µm. **f** Relative cell viability of hPMSC treated and non-treated with neutralizing antibody against RSPO1. **g** Relative cell viability of hPO treated and non-treated with neutralizing antibody against RSPO1. Data are means ± SD ($n = 3$ independent experiments, each performed on samples from five different donors). **g** A two-sided, unpaired Student's t-test was used, ** $p < 0.01$

hPMSC-secreted RSPO proteins are necessary to support hPO culture

So far, we demonstrated that hPMSC were able to sustain the growth of hPO in in vitro culture. However, whether or not the growth of hPO supported by hPMSC was directly related to the production and secretion of specific proteins as the RSPO protein family, was still to be demonstrated. To investigate this hypothesis, ELISA assays for both RSPO1 and RSPO3 were performed, confirming the ability of hPMSC to produce and release these proteins. Since RSPO1 showed higher secretion levels compared to RSPO3 (Fig. 4a, b), we further validated RSPO1 production using qualitative confocal microscopy analysis (Fig. 4c).

Moreover, TOP-FOP supports the ability of pancreatic stromal cells to release factors related to the Wnt canonical pathway (Supplementary Fig. 4).

Furthermore, to corroborate the hypothesis that the hPO growth is directly supported by the RSPO protein secreted by hPMSC, we co-cultured organoids and mesenchymal cells in CC3 medium combined with anti-RSPO1 antibody (Fig. 4d). Interestingly, the growth of hPO was reduced compared to the hPO grown without antibody (Fig. 4e). A metabolic assay confirmed that hPO grown in presence of anti-RSPO1 antibody was significantly reduced, whereas no difference was observed between hPMSC grown in presence of cytokine-specific antibody and in normal co-culture conditions (Fig. 4f, g).

Consistent with the previous results, these data not only unequivocally confirmed that hPMSC were able to sustain the growth of hPO, but also that this ability was strictly related to the competence of hPMSC to produce and release specific proteins such as RSPO proteins.

Discussion

The progress of organoid technology has revolutionized the field of epithelial and cell biology, offering remarkable potential for clinical applications such as the generation of patient-derived organoid biobanks that reliably recapitulate heterogeneity, architecture, physiology and pathophysiology of various tissues and diseases [56]. A pivotal part of this technology is the development of culture media enriched with critical growth factors, particularly R-spondins, which enhance Wnt pathway activity in epithelial stem cells. The R-spondin/Lgr-5 signaling axis plays a crucial role in several self-renewing adult tissues, and most notably, in the digestive tract mucosa. Initial evidence of R-spondin1's role as a growth factor for intestinal epithelial cells, through the activation of canonical Wnt signaling, was demonstrated in a transgenic mouse model with Rspo1 regulated by the immunoglobulin locus [57]. Isolated Lgr5 + intestinal stem cells can be sustained in vitro and stimulated to continuously form organoids [58, 59] with RSPOs being crucial components for these cultures.

Recent studies have demonstrated that, under normal conditions, RSPO expression is primarily localized to non-epithelial stromal components of the niche, such as platelet-derived growth factor receptor–positive stromal cells located within intestinal crypts [60], myofibroblasts positioned proximal to the stem cell compartment in the stomach [61], central vein endothelial cells in the liver [62–64], stromal components of the adrenal gland capsule [65], synovial fibroblasts in osteoarthritis.

The goal of our study was to investigate whether human pancreatic mesenchymal stromal cells could control the proliferative state of pancreatic epithelium regeneration in vitro and to demonstrate that this process is not only influenced by cell-intrinsic plasticity but also by the presence of permissive signals supplied by nonepithelial microenvironment, where Wnt and RSPO cytokines play an important role [66].

Therefore, we investigated whether hPMSC can secrete factors able to impact epithelial cell behavior, specifically studying the release of R-spondin proteins. Our data revealed that hPMSC express transcripts for Gremlin-1, Gremlin-2, Noggin, and all four members of the RSPO family. Bioinformatic analyses further support our findings: by analyzing published single-cell transcriptomic datasets from the human pancreas, we were able to confirm the expression of genes involved in stem cell regulation, tissue homeostasis and regeneration, including Wnt/β-catenin signaling and BMP pathways. The link between the RSPO protein and the BMP antagonists lies in their coordinated regulation of the BMP signaling pathway.

While RSPO proteins potentiate Wnt/β-catenin signaling, the BMP antagonists, including Gremlin-1, Gremlin-2, and Noggin, dampen BMP signaling by blocking the interaction of BMP ligands with their receptors. The pancreas has limited regenerative capacity in adult life but this balance between BMP and Wnt/β-catenin signaling can be involved in pancreatic tissue regeneration after injury and can be useful to improve our understanding of hPMSC role in pancreatic diseases.

With this study we show that pancreatic mesenchymal stromal cells are an essential source of both mitogen molecules RSPO1 and RSPO3 for the human pancreatic epithelial cells in vitro. The results of the TOP-FOP assay suggest that human pancreatic stromal cells are able to produce and release factors linked to the Wnt canonical pathway. Additionally, ELISA assay for RSPO1 and RSPO3 confirmed that hPMSC are able to secrete these proteins, as it has been observed in other stromal cell types [7]. To determine whether these secreted RSPOs could support organoid growth, we examined their biological effects in pancreatic organoid cultures using a non-contact co-culture system of hPMSC and hPO, ensuring experimental conditions were controlled to eliminate potential bias from direct cell interactions. Indeed, our data confirmed that hPMSC can sustain the growth of organoids under these conditions. Furthermore, the immune-sequestration of RSPO1 and RSPO3 shed light on the importance of these factors for the growth of pancreatic organoids. Moreover, its absence within the culture medium drastically reduced the capacity of hPO to survive for long periods.

Our findings indicate the importance of hPMSC in supporting pancreatic cell proliferation and regeneration, specifically identifying RSPO1 and RSPO3 as key secreted factors that influence pancreatic organoid growth. It is well-known that MSC have shown strong potential in the field of regenerative medicine and that they are involved in tissue repair and regeneration. through various mechanisms, for example providing trophic support to damaged tissues and promoting the remodeling of the extracellular matrix and, even in the context of pancreatic diseases [67, 68] and islet transplantation [10, 69–71], it has been shown that MSC support viability, proliferation and function of the epithelial niche.

Recently, with completely different purposes, Ando et al. showed that in mouse and human pancreata, other cell types, such as a subset of pancreatic stellate cells, expressed some levels of R-spondin 3 during pathological conditions like chronic pancreatitis and pancreatic ductal adenocarcinoma [72]. Our study demonstrates that hPMSC in a healthy context also secrete RSPOs, possibly contributing to the regenerative capacity of the pancreatic epithelium. This finding suggests that RSPOs play a broader role in pancreatic homeostasis and regeneration than what was previously understood.

By showing that hPMSC secrete critical factors like RSPO1 and RSPO3, which are key to supporting organoid growth, our work confirms that hPMSC could serve as a stromal component in the construction of more complex 3D models such as assembloids [73] enabling more accurate modeling of tissue architecture, disease progression, and regenerative processes.

Future research should focus on further elucidating the molecular mechanisms underlying RSPO signaling in hPMSC and exploring the potential of these cells in clinical applications for pancreatic disorders.

Supplementary Information The online version contains supplementary material available at https://doi.org/10.1007/s00018-025-05658-0.

Acknowledgements The authors thank Francesco Pampaloni and Meritxell Huch for their scientific support.

Author contributions AC and LL conceived, designed the experiments, and supervised the study. AC, FR and CP supervised the experimental strategy and the data analysis. AC, CP, CM, FR, VP, MB, DT, NE, MCI, FL and VC performed the experiments. AC, CP, MCI and LL wrote the original draft of the manuscript. LP provided the sample collection. LL acquired the funding and administered the project. All authors read the manuscript and approved the final version.

Funding Horizon 2020 Framework Programme, 668350, Lorenza Lazzari, Ministero della Salute.

Data availability All data supporting the findings of this study are available within the paper and its Supplementary Information. Publicly available scRNA-seq datasets were downloaded from the Gene Expression Omnibus (GEO) [48–51].

Declarations

Conflict of interests The authors have no relevant financial or non-financial interests to disclose.

Ethical approval All experiments were performed according to the amended Declaration of Helsinki. The use of human specimens was approved by the Ethical Committee of Fondazione IRCCS Ca' Granda Ospedale Maggiore Policlinico (n° 1982, 14th January 2020) and by the Ethical Committee of IRCCS Ospedale San Raffaele (IPF002-2014, 6th June 2014). Human healthy pancreatic tissues were obtained from the Diabetes Research Institute, IRCCS Ospedale San Raffaele, Milan, Italy from multi-organ donors. The use of human specimens was approved by the Institutional Review Board. Human islets were isolated as previously described [74] at the Pancreatic Islet Processing Unit, a National Transplant Center accredited facility (IT000679) [75].

Consent to publish This study does not contain any individual personal data including any individual's name, images, or videos.

References

1. Campbell JE, Drucker DJ (2015) Islet α cells and glucagon–critical regulators of energy homeostasis. Nat Rev Endocrinol 11:329–338. https://doi.org/10.1038/nrendo.2015.51
2. Grapin-Botton A (2005) Ductal cells of the pancreas. Int J Biochem Cell Biol 37:504–510. https://doi.org/10.1016/j.biocel.2004.07.010
3. Zhou Q, Melton DA (2018) Pancreas regeneration. Nature 557:351–358. https://doi.org/10.1038/s41586-018-0088-0
4. Yamaguchi J, Liss AS, Sontheimer A et al (2015) Pancreatic duct glands (PDGs) are a progenitor compartment responsible for pancreatic ductal epithelial repair. Stem Cell Res 15:190–202. https://doi.org/10.1016/j.scr.2015.05.006
5. Tikhonova AN, Lasry A, Austin R, Aifantis I (2020) Cell-by-cell deconstruction of stem cell niches. Cell Stem Cell 27:19–34. https://doi.org/10.1016/j.stem.2020.06.013
6. Beumer J, Clevers H (2021) Cell fate specification and differentiation in the adult mammalian intestine. Nat Rev Mol Cell Biol 22:39–53. https://doi.org/10.1038/s41580-020-0278-0
7. McCarthy N, Manieri E, Storm EE et al (2020) Distinct mesenchymal cell populations generate the essential intestinal BMP signaling gradient. Cell Stem Cell 26:391-402.e5. https://doi.org/10.1016/j.stem.2020.01.008
8. Greicius G, Kabiri Z, Sigmundsson K et al (2018) PDGFRα+ pericryptal stromal cells are the critical source of Wnts and RSPO3 for murine intestinal stem cells in vivo. Proc Natl Acad Sci U S A 115:E3173–E3181. https://doi.org/10.1073/pnas.1713510115
9. Kim J-E, Fei L, Yin W-C et al (2020) Single cell and genetic analyses reveal conserved populations and signaling mechanisms of gastrointestinal stromal niches. Nat Commun 11:334. https://doi.org/10.1038/s41467-019-14058-5
10. Chmielowiec J, Szlachcic WJ, Yang D et al (2022) Human pancreatic microenvironment promotes β-cell differentiation via non-canonical WNT5A/JNK and BMP signaling. Nat Commun 13:1952. https://doi.org/10.1038/s41467-022-29646-1
11. Kim SK, Hebrok M (2001) Intercellular signals regulating pancreas development and function. Genes Dev 15:111–127. https://doi.org/10.1101/gad.859401
12. Nusse R, Clevers H (2017) Wnt/β-catenin signaling, disease, and emerging therapeutic modalities. Cell 169:985–999. https://doi.org/10.1016/j.cell.2017.05.016
13. Huch M, Bonfanti P, Boj SF et al (2013) Unlimited in vitro expansion of adult bi-potent pancreas progenitors through the Lgr5/R-spondin axis. EMBO J 32:2708–2721. https://doi.org/10.1038/emboj.2013.204
14. de Lau WB, Snel B, Clevers HC (2012) The R-spondin protein family. Genome Biol 13:242. https://doi.org/10.1186/gb-2012-13-3-242
15. Jin Y-R, Yoon JK (2012) The R-spondin family of proteins: emerging regulators of WNT signaling. Int J Biochem Cell Biol 44:2278–2287. https://doi.org/10.1016/j.biocel.2012.09.006
16. Carmon KS, Gong X, Yi J et al (2014) RSPO-LGR4 functions via IQGAP1 to potentiate Wnt signaling. Proc Natl Acad Sci U S A 111:E1221-1229. https://doi.org/10.1073/pnas.1323106111
17. Hao H-X, Xie Y, Zhang Y et al (2012) ZNRF3 promotes Wnt receptor turnover in an R-spondin-sensitive manner. Nature 485:195–200. https://doi.org/10.1038/nature11019
18. Jiang X, Charlat O, Zamponi R et al (2015) Dishevelled promotes Wnt receptor degradation through recruitment of ZNRF3/RNF43 E3 ubiquitin ligases. Mol Cell 58:522–533. https://doi.org/10.1016/j.molcel.2015.03.015
19. Hayat R, Manzoor M, Hussain A (2022) Wnt signaling pathway: a comprehensive review. Cell Biol Int 46:863–877. https://doi.org/10.1002/cbin.11797
20. Schofield R (1978) The relationship between the spleen colony-forming cell and the haemopoietic stem cell. Blood Cells 4:7–25
21. Kitadate Y, Jörg DJ, Tokue M et al (2019) Competition for mitogens regulates spermatogenic stem cell homeostasis in an open niche. Cell Stem Cell 24:79-92.e6. https://doi.org/10.1016/j.stem.2018.11.013
22. Valet M, Narbonne P (2022) Formation of benign tumors by stem cell deregulation. PLoS Genet 18:e1010434. https://doi.org/10.1371/journal.pgen.1010434
23. Szlachcic WJ, Letai KC, Scavuzzo MA, Borowiak M (2023) Deep into the niche: Deciphering local endoderm-microenvironment interactions in development, homeostasis, and disease of pancreas and intestine. BioEssays 45:e2200186. https://doi.org/10.1002/bies.202200186
24. Degirmenci B, Hausmann G, Valenta T, Basler K (2018) Wnt ligands as a part of the stem cell niche in the intestine and the liver. Prog Mol Biol Transl Sci 153:1–19. https://doi.org/10.1016/bs.pmbts.2017.11.011
25. Friedenstein AJ, Petrakova KV, Kurolesova AI, Frolova GP (1968) Heterotopic of bone marrow. Analysis of precursor cells for osteogenic and hematopoietic tissues. Transplantation 6:230–247
26. Morrison SJ, Scadden DT (2014) The bone marrow niche for haematopoietic stem cells. Nature 505:327–334. https://doi.org/10.1038/nature12984
27. Wosczyna MN, Konishi CT, Perez Carbajal EE et al (2019) Mesenchymal stromal cells are required for regeneration and homeostatic maintenance of skeletal muscle. Cell Rep 27:2029-2035.e5. https://doi.org/10.1016/j.celrep.2019.04.074
28. Chu D-T, Phuong TNT, Tien NLB et al (2020) An update on the progress of isolation, culture, storage, and clinical application of human bone marrow mesenchymal stem/stromal cells. Int J Mol Sci 21:708. https://doi.org/10.3390/ijms21030708
29. Bunnell BA (2021) Adipose tissue-derived mesenchymal stem cells. Cells 10:3433. https://doi.org/10.3390/cells10123433
30. Li T, Xia M, Gao Y et al (2015) Human umbilical cord mesenchymal stem cells: an overview of their potential in cell-based therapy. Expert Opin Biol Ther 15:1293–1306. https://doi.org/10.1517/14712598.2015.1051528
31. Barilani M, Lavazza C, Boldrin V et al (2016) A chemically defined medium-based strategy to efficiently generate clinically relevant cord blood mesenchymal stromal colonies. Cell Transplant 25:1501–1514. https://doi.org/10.3727/096368916X690827
32. Barilani M, Peli V, Cherubini A et al (2019) NG2 as an identity and quality marker of mesenchymal stem cell extracellular vesicles. Cells 8:1524. https://doi.org/10.3390/cells8121524
33. Caplan AI, Correa D (2011) The MSC: an injury drugstore. Cell Stem Cell 9:11–15. https://doi.org/10.1016/j.stem.2011.06.008
34. Kalinina N, Kharlampieva D, Loguinova M et al (2015) Characterization of secretomes provides evidence for adipose-derived mesenchymal stromal cells subtypes. Stem Cell Res Ther 6:221. https://doi.org/10.1186/s13287-015-0209-8
35. Caplan AI, Dennis JE (2006) Mesenchymal stem cells as trophic mediators. J Cell Biochem 98:1076–1084. https://doi.org/10.1002/jcb.20886
36. Kou X, Liu J, Wang D et al (2022) Exocrine pancreas regeneration modifies original pancreas to alleviate diabetes in mouse

models. Sci Transl Med 14:9170. https://doi.org/10.1126/scitranslmed.abg9170
37. Schneider G, Saur D (2011) Mesenchymal stem cells: therapeutic potential for acute pancreatitis. Gastroenterology 140:779–782. https://doi.org/10.1053/j.gastro.2011.01.026
38. Sordi V, Melzi R, Mercalli A et al (2010) Mesenchymal cells appearing in pancreatic tissue culture are bone marrow-derived stem cells with the capacity to improve transplanted islet function. Stem Cells 28:140–151. https://doi.org/10.1002/stem.259
39. Dossena M, Piras R, Cherubini A et al (2020) Standardized GMP-compliant scalable production of human pancreas organoids. Stem Cell Res Ther 11:94. https://doi.org/10.1186/s13287-020-1585-2
40. Cherubini A, Rusconi F, Lazzari L (2021) Identification of the best housekeeping gene for RT-qPCR analysis of human pancreatic organoids. PLoS ONE 16:e0260902. https://doi.org/10.1371/journal.pone.0260902
41. Boj SF, Hwang C-I, Baker LA et al (2015) Organoid models of human and mouse ductal pancreatic cancer. Cell 160:324–338. https://doi.org/10.1016/j.cell.2014.12.021
42. Loomans CJM, Williams Giuliani N, Balak J et al (2018) Expansion of adult human pancreatic tissue yields organoids harboring progenitor cells with endocrine differentiation potential. Stem Cell Reports 10:712–724. https://doi.org/10.1016/j.stemcr.2018.02.005
43. Dominici M, Le Blanc K, Mueller I et al (2006) Minimal criteria for defining multipotent mesenchymal stromal cells. The International Society for Cellular Therapy position statement. Cytotherapy 8:315–317. https://doi.org/10.1080/14653240600855905
44. Horwitz EM, Le Blanc K, Dominici M et al (2005) Clarification of the nomenclature for MSC: The International Society for Cellular Therapy position statement. Cytotherapy 7:393–395. https://doi.org/10.1080/14653240500319234
45. Angelova PR, Barilani M, Lovejoy C et al (2017) Mitochondrial dysfunction in Parkinsonian mesenchymal stem cells impairs differentiation. Redox Biol 14:474–484. https://doi.org/10.1016/j.redox.2017.10.016
46. Georgakopoulos N, Prior N, Angres B et al (2020) Long-term expansion, genomic stability and in vivo safety of adult human pancreas organoids. BMC Dev Biol 20:4. https://doi.org/10.1186/s12861-020-0209-5
47. Broutier L, Andersson-Rolf A, Hindley CJ et al (2016) Culture and establishment of self-renewing human and mouse adult liver and pancreas 3D organoids and their genetic manipulation. Nat Protoc 11:1724–1743. https://doi.org/10.1038/nprot.2016.097
48. Lawlor N, George J, Bolisetty M et al (2017) Single-cell transcriptomes identify human islet cell signatures and reveal cell-type-specific expression changes in type 2 diabetes. Genome Res 27:208–222. https://doi.org/10.1101/gr.212720.116
49. Segerstolpe Å, Palasantza A, Eliasson P et al (2016) Single-cell transcriptome profiling of human pancreatic islets in health and Type 2 diabetes. Cell Metab 24:593–607. https://doi.org/10.1016/j.cmet.2016.08.020
50. Grün D, Muraro MJ, Boisset J-C et al (2016) De novo prediction of stem cell identity using single-cell transcriptome data. Cell Stem Cell 19:266–277. https://doi.org/10.1016/j.stem.2016.05.010
51. Muraro MJ, Dharmadhikari G, Grün D et al (2016) A single-cell transcriptome atlas of the human pancreas. Cell Syst 3:385-394.e3. https://doi.org/10.1016/j.cels.2016.09.002
52. Butler A, Hoffman P, Smibert P et al (2018) Integrating single-cell transcriptomic data across different conditions, technologies, and species. Nat Biotechnol 36:411–420. https://doi.org/10.1038/nbt.4096
53. Stuart T, Butler A, Hoffman P et al (2019) Comprehensive integration of single-cell data. Cell 177:1888-1902.e21. https://doi.org/10.1016/j.cell.2019.05.031
54. Viswanathan S, Shi Y, Galipeau J et al (2019) Mesenchymal stem versus stromal cells: International Society for Cell & Gene Therapy (ISCT®) Mesenchymal Stromal Cell committee position statement on nomenclature. Cytotherapy 21:1019–1024. https://doi.org/10.1016/j.jcyt.2019.08.002
55. Driehuis E, van Hoeck A, Moore K et al (2019) Pancreatic cancer organoids recapitulate disease and allow personalized drug screening. Proc Natl Acad Sci U S A 116:26580–26590. https://doi.org/10.1073/pnas.1911273116
56. van de Wetering M, Francies HE, Francis JM et al (2015) Prospective derivation of a living organoid biobank of colorectal cancer patients. Cell 161:933–945. https://doi.org/10.1016/j.cell.2015.03.053
57. Kim K-A, Kakitani M, Zhao J et al (2005) Mitogenic influence of human R-spondin1 on the intestinal epithelium. Science 309:1256–1259. https://doi.org/10.1126/science.1112521
58. Sato T, Vries RG, Snippert HJ et al (2009) Single Lgr5 stem cells build crypt-villus structures in vitro without a mesenchymal niche. Nature 459:262–265. https://doi.org/10.1038/nature07935
59. Barker N, Huch M, Kujala P et al (2010) Lgr5(+ve) stem cells drive self-renewal in the stomach and build long-lived gastric units in vitro. Cell Stem Cell 6:25–36. https://doi.org/10.1016/j.stem.2009.11.013
60. Kabiri Z, Greicius G, Madan B et al (2014) Stroma provides an intestinal stem cell niche in the absence of epithelial Wnts. Development 141:2206–2215. https://doi.org/10.1242/dev.104976
61. Sigal M, Logan CY, Kapalczynska M et al (2017) Stromal R-spondin orchestrates gastric epithelial stem cells and gland homeostasis. Nature 548:451–455. https://doi.org/10.1038/nature23642
62. Cordero-Espinoza L, Dowbaj AM, Kohler TN et al (2021) Dynamic cell contacts between periportal mesenchyme and ductal epithelium act as a rheostat for liver cell proliferation. Cell Stem Cell 28:1907-1921.e8. https://doi.org/10.1016/j.stem.2021.07.002
63. Planas-Paz L, Orsini V, Boulter L et al (2016) The RSPO-LGR4/5-ZNRF3/RNF43 module controls liver zonation and size. Nat Cell Biol 18:467–479. https://doi.org/10.1038/ncb3337
64. Rocha AS, Vidal V, Mertz M et al (2015) The angiocrine factor rspondin3 is a key determinant of liver zonation. Cell Rep 13:1757–1764. https://doi.org/10.1016/j.celrep.2015.10.049
65. Vidal V, Sacco S, Rocha AS et al (2016) The adrenal capsule is a signaling center controlling cell renewal and zonation through Rspo3. Genes Dev 30:1389–1394. https://doi.org/10.1101/gad.277756.116
66. Murtaugh LC, Kopinke D (2008) Pancreatic stem cells. In: StemBook. Harvard Stem Cell Institute, Cambridge (MA)
67. Ahmed SM, Morsi M, Ghoneim NI et al (2018) Mesenchymal stromal cell therapy for pancreatitis: a systematic review. Oxid Med Cell Longev 2018:3250864. https://doi.org/10.1155/2018/3250864
68. Taha HS, Moustafa EM, Moawed FS, Hegazy MG (2021) Curative role of mesenchymal stromal cells in chronic pancreatitis: modulation of MAPK and TGF-β1/SMAD factors. Int J Immunopathol Pharmacol 35:20587384211054036. https://doi.org/10.1177/20587384211054036
69. Barachini S, Biso L, Kolachalam S et al (2023) Mesenchymal stem cell in pancreatic islet transplantation. Biomedicines 11:1426. https://doi.org/10.3390/biomedicines11051426
70. Khatri R, Petry SF, Linn T (2021) Intrapancreatic MSC transplantation facilitates pancreatic islet regeneration. Stem Cell Res Ther 12:121. https://doi.org/10.1186/s13287-021-02173-4
71. Koehler N, Buhler L, Egger B, Gonelle-Gispert C (2022) Multipotent mesenchymal stromal cells interact and support islet of langerhans viability and function. Front Endocrinol (Lausanne) 13:822191. https://doi.org/10.3389/fendo.2022.822191
72. Ando R, Shiraki Y, Miyai Y et al (2024) Meflin is a marker of pancreatic stellate cells involved in fibrosis and epithelial regeneration

in the pancreas. J Pathol 262:61–75. https://doi.org/10.1002/path.6211
73. Lin M, Hartl K, Heuberger J et al (2023) Establishment of gastrointestinal assembloids to study the interplay between epithelial crypts and their mesenchymal niche. Nat Commun 14:3025. https://doi.org/10.1038/s41467-023-38780-3
74. Melzi R, Piemonti L, Nano R et al (2004) Donor and isolation variables associated with human islet monocyte chemoattractant protein-1 release. Transplantation 78:1564–1567. https://doi.org/10.1097/01.tp.0000144184.20085.41
75. EU Coding Platform. https://webgate.ec.europa.eu/eucoding/reports/te/index.xhtml. Accessed 17 Jul 2024